Diffusive and non-diffusive contributions to momentum transport in AUG experiments and the European intrinsic rotation database

R. M. McDermott[1], T. Odstrcil[1], C. Angioni[1], B. P. Duval[2], A. N. Karpushov[2], R. Fischer[1], A. Salmi[3], T. Tala[3], G. Tardini[1], E. Viezzer[1] and the ASDEX Upgrade Team

[1]*Max-Planck-Institut für Plasmaphysik, Garching, Germany* [2] *Ecole Polytechnique Federale de Lausanne (EPFC), Centre de Recherches en Physique des Plasmas, Station 13*
[3]*VTT, P.O. Box 1000, FIN-02044 VTT, FInland*

Introduction

Momentum transport has become an active area of research within the tokamak community due to the realization that significant rotation and rotation shear is needed to tame turbulent transport and ensure plasma stability. Moreover, knowledge of the rotation profile is needed to predict impurity particle transport. As such, the goal of the rotation community is to gain a fundamental understanding of the sources, sinks and transport of momentum in fusion plasmas in order to accurately predict the rotation profiles. At ASDEX Upgrade (AUG) significant effort has been dedicated to this via a wide variety of experimental techniques.

Database analysis of type-I ELMy H-mode plasmas

One such technique, a profile database approach pioneered by Weisen *et al* [1, 2], is able to disentangle the diffusive momentum flux from all of the non-diffusive fluxes. This approach has an advantage over traditional torque modulation analyses in that it does not have to assume a negligible residual stress. It does, however, require the non-diffusive transport within the dataset to be similar, as it returns only a single averaged non-diffusive flux profile. The approach employs a momentum conservation equation re-written in a linear form ($y = mx + b$) such that the unknowns are encapsulated entirely in the slope and the offset.

$$\frac{R}{L_\omega} = \frac{R}{\omega_\phi}\frac{\partial \omega_\phi}{\partial r} = \frac{\chi_i}{\chi_\phi}\left(\frac{R\Pi_\phi}{n_i m_i R \chi_i \omega_\phi} + \frac{R\Gamma_n}{\chi_i n_i}\right) + \left(\frac{Rv_\phi}{\chi_\phi} + \frac{R\Pi_{RS}}{n_i m_i R \chi_\phi}\right) \quad (1)$$

In Eqn. 1 the left hand side is the normalised gradient of the toroidal rotation frequency (R/L_ω), which can be obtained directly from measurements. The first set of brackets on the right hand side contains the normalised NBI torque and the particle flux ($t^* + \Gamma_n^*$), both of which can be calculated from transport codes such as TRANSP. There remain only two unknowns: the Prandtl number, $P_r = \chi_\phi/\chi_i$, which is the inverse of the slope in equation 1, and the non-diffusive contributions (the pinch number $V_N = RV_\phi/\chi_\phi$ and the normalised residual stress momentum flux Π_{RS}^*), which together correspond to the y-intercept.

Using this equation and a sufficiently large and varied database of observations, an averaged Prandtl and pinch number profile can be obtained by applying linear fits to the dataset at multiple radial locations. This is illustrated for one radial position on the left-hand side of Fig. 1 for a database of steady, NBI-heated, AUG H-mode plasmas [3]. Here, the measured R/L_ω is plotted against the normalised NBI torque. The dashed line corresponds to the case of $P_r = 1$ and zero non-diffusive flux. The vertical offset of the data points from this line clearly demonstrates the presence of a non-diffusive flux. The blue shaded region indicates the uncertainty in the analysis and translates directly to the error bars shown in Fig. 1b. Here, the profiles of the resultant non-diffusive momentum flux and Prandtl number are shown. The Prandtl number is approximately 1 everywhere (within the error bars), while the non-diffusive flux is small in the core and increases toward the edge, qualitatively consistent with a Coriolis momentum pinch [4]. However, the pinch numbers obtained from GKW, quasi-linear, gy-

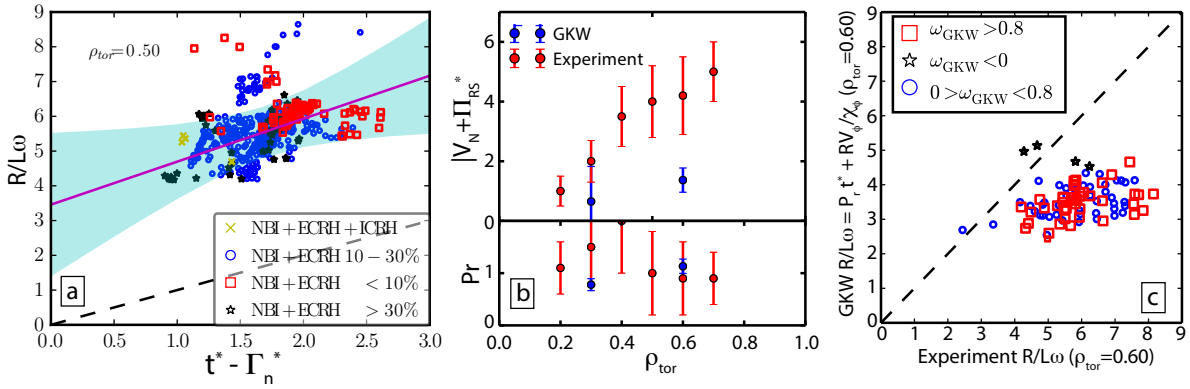

Figure 1: (left) Normalised toroidal rotation gradient vs. the normalised torque plus particle flux for a database of NBI heated AUG H-mode plasmas at ρ_ϕ =0.5. (right) Profile of the non-diffusive momentum flux derived from the linear analysis plus the pinch numbers calculated by GKW at two radial positions.

rokinetic simulations at $k_y\rho_i = 0.3$ of a representative subset of the database are significantly smaller than the experimentally determined flux. The resulting GKW predicted rotation gradients are a factor of two smaller than the experimentally measured values. This can be seen in Fig. 1c where the R/L_ω values predicted by GKW (the sum of the diffusive and convective fluxes) at $\rho_{tor} = 0.6$ are plotted against the experimentally measured values. This discrepancy suggests the presence of a co-current directed residual stress momentum flux to resolve the difference. Unfortunately, within the uncertainties of the measurements, nothing quantitative can be concluded.

It is potentially possible to gain information on the physics at play by looking at the parameter dependences of the experimental and theoretical data. To this end, the experimental R/L_ω data between $\rho_\phi = 0.2$ and 0.7 were regressed against the parameters found to be relevant in an analogous work performed for a database of JET discharges [2].

$$R/L_\omega = 0.6(t^* - \Gamma_n^*) - 0.9T_e/T_i - 0.3q + 19\epsilon^{\frac{1}{2}} - 0.5 \quad (2)$$

The standard deviations associated with the regression variables are $[0.1, 0.3, 0.1, 2, 0.7]$. Unsurprisingly, the radial coordinate $\epsilon = r/R$ is the most relevant parameter in the regression followed by the diffusive contribution to the transport (applied torque), T_e/T_i and the safety factor q. In contrast to the JET results, $R/L_{\rm ne}$ is not found to be important in this regression. However, if ϵ is removed from the regression and the data at individual radii examined, then R/L_{ne} becomes the second most statistically relevant parameter after the applied torque. A dependence of R/L_ω on R/L_{ne} is expected due to the contribution of the Coriolis momentum pinch [4]. Indeed, in the regressions of the GKW predicted pinch numbers, this dependence shows up clearly. The lack of an R/L_{ne} dependence in the experimental R/L_ω when ϵ is included is, perhaps, not too surprising given that the GKW results under-predict the measured rotation gradients by a factor of two; i.e. the missing half of the non-diffusive flux may exhibit a different ϵ (and other) dependence that masks the contribution. Taken together, this data indicates that there is a significant, non-diffusive, co-current directed, momentum flux that is not taken into account in the modeling. This is qualitatively consistent with the evidence for a co-current intrinsic torque in NBI heated plasmas at DIII-D [5].

Comparison of ASDEX Upgrade and TCV intrinsic rotation profiles

Given that intrinsically driven momentum fluxes can play a significant role in determining the rotation in fusion plasmas, it is important to gain a better understanding of the mechanisms

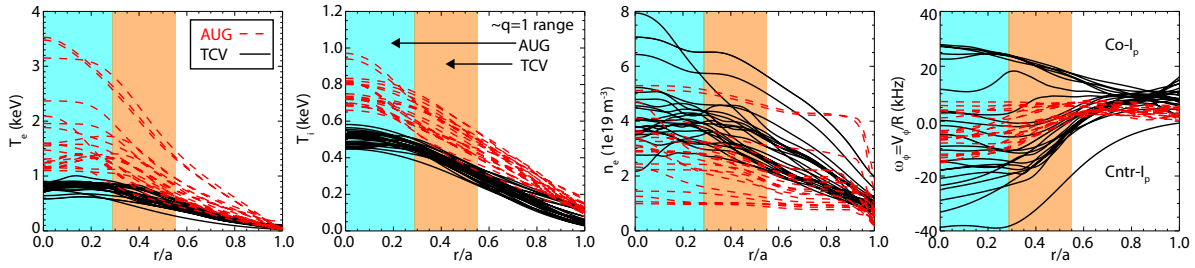

Figure 2: Electron and ion temperature, electron density and intrinsic toroidal rotation profiles from TCV (black solid) and AUG (red dashed) LSN, favorable drift, positive triangularity Ohmic L-mode discharges.

driving these fluxes and their dependences on plasma parameters. Work in this direction has been performed at AUG which showed that the intrinsic rotation is strongly linked to the electron density gradient and to the plasma density and temperature through the collisionality [6, 7]. More recently, through the framework of the European intrinsic rotation database, AUG and TCV intrinsic rotation data from Ohmic L-mode plasmas have been compared for the first time using the same analysis tools and methodologies. The AUG dataset is limited to LSN, favourable drift discharges with positive upper and lower triangularity, which is also the planned ITER configuration. Only TCV profiles from plasmas matching these criteria were used for the comparison, limiting the TCV dataset to 23 samples. For the AUG data, a subset of 20 samples that spanned the available parameter space was selected. The plasma profiles corresponding to the selected samples are shown in Fig. 2. The electron and ion temperatures tend to be higher in the AUG dataset. This is partly explained by the higher plasma currents and partly by the AUG data extending to a lower density range.

Interestingly, the toroidal velocity profiles (not shown) from the two machines are, at first glance, remarkably similar. They both display co-current edge rotations of roughly 10km/s and demonstrate a wide variety of profile shapes in the plasma core resulting in central toroidal rotations between -20 and +20km/s. However, the toroidal rotation frequency profiles (right hand side of Fig. 2), which account for machine size, show differences. The TCV profiles cover a wider range in ω and, more importantly, a wider range in the normalised toroidal rotation gradient, $u' = -(R^2/v_{th,i})\, d\omega/dr$, where $v_{th,i} = \sqrt{2T_i/m_i}$ is the main ion thermal velocity. The profiles display other differences. The "flattening" point of the profile, i.e. the point inside of which the gradient is effectively zero, differs between the two devices as a function of r/a, ρ_{tor} and ρ_ψ. The region of steep rotation gradient for the AUG profiles extends further inside ($0.25 < r/a < 0.65$) compared to TCV ($0.45 < r/a < 0.65$). The hypothesis that the flattening of the profiles, hence the limiting of the gradient region, is caused by sawteeth is supported by the relative positions of the q=1 surfaces, see Fig. 2. The rather large difference in q=1 surface position persists even for plasmas with similar q_{95} values. The TCV dataset includes q_{95} values between 2.7 and 4.9, while the AUG data ranges between 3.7 and 8.5, providing only a small region of overlap around $q_{95} = 4$. However, if the aspect ratio difference between the two devices ($\bar{\epsilon} = 0.31$ for AUG and 0.26 for TCV) is taken into account, the positional agreement of the q=1 surfaces in terms of ϵ improves and one finds that the regions of strongest rotation gradient overlap between $0.1 < \bar{\epsilon} < 0.175$.

A comparison of the parameter dependences of the observed rotation gradients in this ϵ region yields encouragingly similar results. In Fig. 3 the normalised rotation gradients from TCV and AUG are shown as a function of the dominant parameter dependences found in [7] as well as ρ^*. With the exception of a small group of points with positive rotation gradients (co-I_p profiles), the data from the two machines overlay quite well. The trend with R/L_{ne}

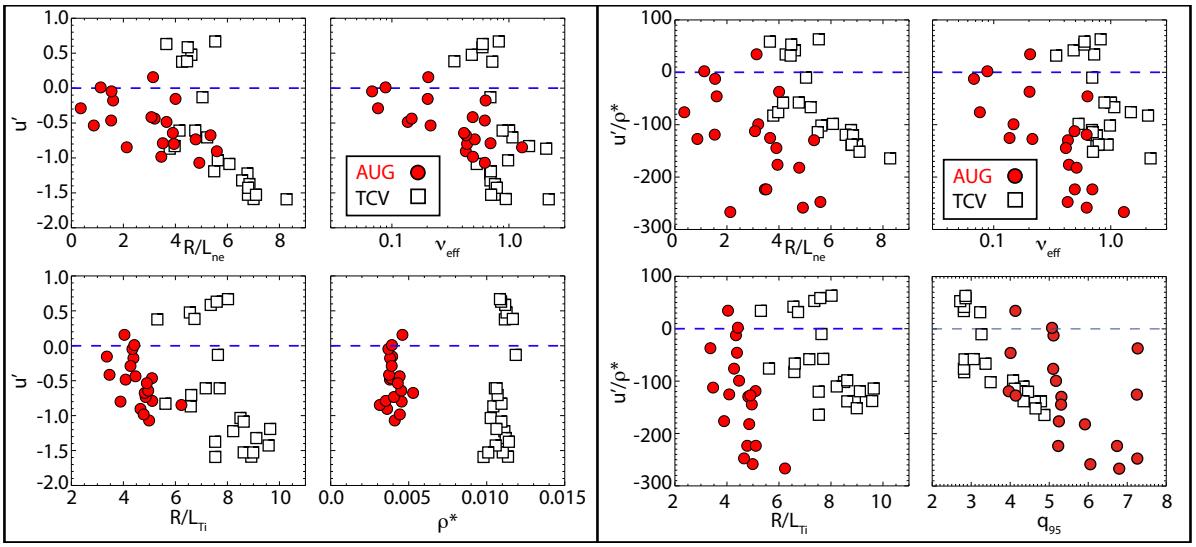

Figure 3: Parameter dependences of u' (left) and u'/ρ^* (right) averaged over $0.1 < \epsilon < 0.175$.(right)

is particularly striking. These datasets also show strong trends with other parameters such as q_{95}, that is itself strongly correlated with R/L_{ne} (not shown). Most core localised residual stress momentum fluxes are expected to scale with ρ^*. In Fig. 3 it is clear that the available range of ρ^* from either machine is too small to see any kind of scaling. Together though, the data spans over a factor of two in ρ^*. Multi-variable regressions of the combined datasets that include ρ^* always yield ρ^* as the dominant parameter dependence with a positive coefficient, and explain the co-current TCV rotation points as having the highest ρ^* combined with the lowest normalised gradients, all of which have negative coefficients. These co-current points cause the regressions with ρ^* to have a lower RMSE error than those without.

However, one would expect the magnitude of the residual stress, Π_{RS}, to scale as ρ^* multiplied by some function with other parameter dependences, i.e. $\Pi_{RS} \sim \rho^* F\left(R/L_{ne}, R/L_{Ti}, ...\right)$. In this analysis, as u' is being used as a proxy for Π_{RS}, we would expect u'/ρ^* to demonstrate the residual stress parameter dependences more clearly than u' alone. Accordingly, the u'/ρ^* values of the database were also examined and regressed. The right hand side of Fig. 3 shows the results for the same subset of parameters. This normalisation significantly reduces the previously observed correlations, although it improves the correlation of the data with q_{95}, shown only for the u'/ρ^* dataset. Additionally, the ability of a regression to reproduce the experimental u'/ρ^* is not improved over u' alone. Based on the analyses performed thus far on the combined AUG and TCV datasets, there is no clear evidence of a dominant ρ^* dependence in the intrinsic rotation. Ideally, the intrinsic rotation profiles between the two machines should be compared at matched dimensionless parameters (excluding ρ^*). Unfortunately, this data does not yet exist within the database, but will be the focus of future experimental effort.

References

[1] H. Weisen et al, Nucl. Fusion 52, 042001 (2012)
[2] H. Weisen et al, Nucl. Fusion 52, 114024 (2012)
[3] T. Odstrcil, Masters Thesis University of Stuttgart (2013)
[4] A. G. Peeters et al, Phys. Rev. Lett. 98, 265003 (2007)
[5] W. Solomon et al, Nucl. Fusion 49, 085005 (2009)
[6] C. Angioni et al, Phys. Rev. Lett. 107, 215003 (2011)
[7] R.M. McDermott et al, Nucl. Fusion 54, 043009 (2014)

Acknowledgements: This work has been carried out within the framework of the EUROfusion Consortium and has received funding from the Euratom research and training programme 2014-2018 under grant agreement No 633053. The views and opinions expressed herein do not necessarily reflect those of the European Commission.